formula $\sigma^2 = (1/V)^2 \sum \sigma^2(F_o)$ is used (Cruickshank, 1949). When the estimate is based on variations between chemically equivalent regions in the molecule, a slightly larger value of 0.05 e Å^{-3} is obtained.

References

BLESSING, R. H. (1986a). J. Appl. Cryst. 19, 412.
BLESSING, R. H. (1986b) Cryst. Rev. 1, 1.
COPPENS, P., LEISEROWITZ, L. & RABINOVICH, D. (1965). Acta Cryst. 18, 1035–1038.
CRUICKSHANK, D. W. J. (1949). Acta Cryst. 2, 65–70.
DUNITZ, J. D. & WHITE, D. N. J. (1973). Acta Cryst. A29, 93–96.
GEIGER, D. K., LEE, Y. J. & SCHEIDT, W. R. (1984). J. Am. Chem. Soc. 106, 6339–6343.
HANSEN, N. K. & COPPENS, P. (1978). Acta Cryst. 34, 909–921.
HIRSHFELD, F. L. (1976). Acta Cryst. A32, 239–244.
International Tables for X-ray Crystallography (1974). Birmingham: Kynoch Press. (Present distributor D. Reidel, Dordrecht.)
LECOMTE, C., BLESSING, R. H., COPPENS, P. & TABARD, A. (1986). J. Am. Chem. Soc. 108, 6942–6950.
LEHMANN, M. S. & LARSEN, F. K. (1974). Acta Cryst. A30, 580–584.
MCMULLAN, R. K., EPSTEIN, J., RUBLE, J. R. & CRAVEN, B. M. (1979). Acta Cryst. B35, 688–691.
MOTHERWELL, S. (1979). PLUTO. Program for plotting molecular and crystal structures. Univ. of Cambridge, England.
SCHEIDT, W. R. & CHIPMAN, D. M. (1986). J. Am. Chem. Soc. 108, 1163–1167.
SCHEIDT, W. R., KIRNER, J. F., HOARD, J. L. & REED, C. A. (1987). J. Am. Chem. Soc. 109, 1963–1968.
SHOMAKER, V. & TRUEBLOOD, K. N. (1968). Acta Cryst. B24, 63–76.

Electron Density in Potassium Bis(dithiooxalato-S,S')nickelate(II)

BY E. N. MASLEN AND N. SPADACCINI

Crystallography Centre, University of Western Australia, Nedlands, Western Australia 6009, Australia

Abstract

At room temperature, $K_2[Ni(C_2O_2S_2)_2]$ is: monoclinic, $P2_1/c$, $M_r = 377.2$, $a = 11.044$ (2), $b = 4.1949$ (7), $c = 13.404$ (2) Å, $\beta = 118.13$ (1)°, $V = 547.6$ (2) Å^3, $Z = 2$, $D_x = 2.29$ Mg m^{-3}, Mo $K\alpha$, $\lambda = 0.71069$ Å, $\mu = 3.34$ mm^{-1}, $F(000) = 372$, $T = 298$ K, $R = 0.053$ and $wR = 0.027$ for 3943 reflections. The nickel coordinates with sulfur rather than oxygen in a structure which may be regarded either as square planar or as strongly distorted octahedral. To assist in understanding the structural behaviour of the system, the electron density has been analysed. For these metal–sulfur bonds, the electron density polarizes far less than it does in metal–fluorine or metal–oxygen bonds. The extent of the depletion of the nickel $3d$ subshell is related to the electronegativity of the ligand atom. The overlap of atomic densities is expected to result in only moderate electron movement for sulfur ligands, which are weakly electronegative. There is a net transfer of electrons towards the nickel, and the negative charge associated with the $[Ni(S_2C_2O_2)_2]$ anion resides predominantly on that atom.

Introduction

The change in atomic polarizability through the first-transition-metal series has been observed experimentally in difference density maps. In the compounds KMF_3, where $M = $ Mn, Fe, Co and Ni with octahedral coordination (Kijima, Tanaka & Marumo, 1981, 1983; Miyata, Tanaka & Marumo, 1983), the depletion of the sum of the atomic densities along the M—F bonds rises steadily through the series. The increase in population of the valence subshell of the central atom results in greater spin conflict with the electrons in the valence subshell of the strongly electronegative F atoms.

As a consequence of the Pauli (1925) principle there is a transfer of density away from the overlap region. The effect would maximize for $KCuF_3$ except that the system becomes unstable, changing to structures which are elongated octahedra, or even square planar. This effect for Cu^{II} compounds is understood in terms of the Jahn–Teller theorem. For transition metals lighter than nickel, square-planar complexes are formed only when strong steric constraints are imposed on the ligands. For Ni^{II} compounds, on the

other hand, square-planar complexes may be obtained without steric constraints provided the ligands are not strongly electronegative. For strongly electronegative ligands such as fluorine the depletion of the electron density along the nickel–ligand bonds is large. The effect of the less-electronegative ligands on that density was studied as a guide to understanding the nature of square-planar Ni[II] compounds.

Experimental

Potassium bis(dithiooxalato-*S,S'*)nickelate(II) is a square-planar structure with the central atom bonded to S atoms. The compound was synthesized from equal weights of potassium dithiooxalate and nickel sulfate in solution (Jones & Tasker, 1909). It crystallizes either as needles or as bypyramidal octahedra (Robinson & Jones, 1912), indicating dimorphism with a transition temperature of approximately 293 K. The dimorphism was supposedly discounted by Cox, Wardlaw & Webster (1935) by an X-ray structure analysis. The structure of a red form of $K_2[Ni(S_2C_2O_2)_2]$ was further refined (Coucouvanis, Baenziger & Johnson, 1973) but the question of dimorphism was not addressed. A new black form of $K_2[Ni(S_2C_2O_2)_2]$ which has a structure very different to that of the above red form was reported by Gleizes, Clery, Bruniquel & Cassoux (1979).

Crystals of the black form of $K_2[Ni(S_2C_2O_2)_2]$ were obtained by allowing a hot solution of potassium dithiooxalate and nickel sulfate to cool to room temperature. The crystals were prismatic parallelepipeds, elongated along **b**, with sharply defined faces. The crystal chosen for data collection had dimensions $0.18 \times 0.07 \times 0.14$ mm bounded by the faces $\pm(\bar{1}11)$, $\pm(10\bar{3})$ and $\pm(100)$.

The crystal was oriented on a Syntex $P2_1$ diffractometer using Mo $K\alpha$ radiation. The standard cell setting with space group $P2_1/c$ was preferred to that of Gleizes *et al.* (1979). Experimental details are given in Table 1. One hemisphere to the limit of $(\sin \theta)/\lambda \leq 0.95$ Å^{-1} and another hemisphere to the limit of $(\sin \theta)/\lambda \leq 0.59$Å^{-1}, totalling 10 840 reflections, were measured. The data were corrected for absorption analytically (Alcock, 1974), sorted and merged, resulting in 3943 independent reflection intensities.

The initial position parameters were taken from the structure analysis of Gleizes *et al.* (1979), transformed in accordance with the different choice of cell. All variable positions, anisotropic thermal parameters and a scale factor were refined by full-matrix least squares (based on F). The spherically averaged atomic form factors were those of Cromer & Mann (1968), with corrections for anomalous dispersion by Cromer & Liberman (1970). The least-squares weights were $1/\sigma^2(F)$. The final refinement gave no indication of extinction, and any attempt to refine an isotropic extinction parameter (Larson, 1970) gave unphysical

Table 1. *Experimental and refinement data*

Diffractometer	Syntex $P2_1$
Monochromator	Graphite
Scan type	$\omega/2\theta$
Scan speed (° s^{-1}) min.	0.065
max.	0.488
Scan width $(a + b \tan \theta)$ (°)	1.55; 0.70
Max 2θ (°)	85
Maximum variation in intensity of standards	
± 400 ± 040 ± 006 (%)	3
Number of reflections measured	10 840
Transmission range in absorption corrections	0.59–0.75
R_{int} (before and after absorption)	0.023; 0.021
Number of independent reflections	
$(0 \leq h \leq 21, 0 \leq k \leq 7, -25 \leq l \leq 22)$	3943
R	0.053
wR	0.027
GoF	1.80 (2)
Weights	$1/\sigma^2 (F)$
Final max. shift/e.s.d.	0.001
Max. height in final difference Fourier synthesis (e Å^{-3})	0.62
Min. height in final difference Fourier synthesis (e Å^{-3})	-0.72

Table 2. *Fractional positional coordinates and equivalent isotropic temperature factors (Å^2) with e.s.d.'s in parentheses*

	x	y	z	U_{eq}* ($\times 10^5$)
Ni	0	0	0	2500
K	0.37198 (3)	0.20439 (7)	0.33985 (2)	3194
S(1)	0.15438 (3)	-0.28690 (8)	0.13617 (3)	3165
S(2)	0.12176 (3)	0.01588 (9)	-0.08974 (3)	3232
O(1)	0.3895 (1)	-0.4942 (3)	0.16096 (9)	4632
O(2)	0.36577 (9)	-0.2146 (2)	-0.02903 (8)	3299
C(1)	0.2846 (1)	-0.3414 (3)	0.1023 (1)	2863
C(2)	0.2693 (1)	-0.1863 (3)	-0.00722 (9)	2540

$$* \ U_{eq} = (1/6\pi^2) \sum_i \sum_j \beta_{ij} \mathbf{a}_i . \mathbf{a}_j.$$

negative values for r^*. The final R and wR factors were 0.053 and 0.027 with a GoF value of 1.80 (2). The refinement details are included in Table 1 and the final position parameters are given in Table 2.[†] All calculations were performed on a Perkin–Elmer 3240 computer using the *XTAL* system (Stewart & Hall, 1983).

Structural geometry

Bond distances and angles are given in Fig. 1. The structure contains $[Ni(S_2C_2O_2)_2]$ moieties stacked parallel to the **b** axis with the Ni atoms separated by the **b** lattice parameter. The K atoms are in tunnels between the $[Ni(S_2C_2O_2)_2]$ planes and stacked parallel to the **b** axis, with the K—S and K—O contacts providing structural cohesion. The K atom is surrounded by five O atoms [contact distances ranging from 2.725 (1) to 2.830 (1) Å] and three S atoms [contact distances ranging from 3.3600 (5) to

3·5160 (7) Å]. The Ni atom is surrounded by four K atoms at distances of 4·5516 (6) and 5·5786 (6) Å and two Ni atoms displaced along the **b** axis [4·1949 (7) Å]. The coordination polyhedron is irregular. The maximum deviation from the least-squares plane for the [Ni(S₂C₂O₂)₂] unit is 0·075 (1) Å. The plane normal makes an angle of 33·32 (2)° with the **b** axis and the perpendicular distance between planes is 3·505 (1) Å. This packing is similar to that for sodium and lithium bis(dithiooxalato-*S,S'*)nickelate(II), where the angles (30 and 28°), the Ni–Ni spacings (3·785 and 3·666 Å) and the interplane distances (3·28 and 3·24 Å) are decreased (Maury & Gleizes, 1980). A divalent cation in the barium analogue of this compound changes the packing to a zig-zag formation (Gleizes, Maury, Cassoux & Galy, 1981).

The immediate environment of the Ni atom is square planar, with bond distances of 2·1800 (4) and 2·1875 (5) Å and angles of 87·92 (2) and 92·08 (2)°. However, the coordination is pseudo octahedral when the cell packing is considered. The short distance between planar moieties brings the S(1) atoms bonded to the Ni atoms at (0, 1, 0) and (0, −1, 0) directly above and below the Ni atom at the origin as illustrated in Fig. 2. The longest Ni–S distance is 3·5003 (5) Å. The angles subtended at the Ni atom between the S atoms at the octahedral positions and the S atoms in the NiS₄ plane are 92·23 (2) and 90·79 (2)°.

The symmetry of the ideal nickel dithiooxalate molecule is higher than the crystallographic sym-

metry. In the crystal the molecule has pseudo *mm* symmetry with the mirror planes perpendicular to the plane of the molecule and bisecting the S(1)—Ni—S(2) angles.

Difference density

The difference density was evaluated. Relevant sections are shown in Figs. 3 and 4. The S—C bonds are essentially devoid of features. The difference densities along the C—C and C—O bonds are consistent with those reported for similar bonds in related structures (*e.g.* Dunitz & Seiler, 1983; Coppens, Boehme, Price & Stevens, 1981; Becker, 1977; and references therein). There are small peaks along the C(1)—C(2) and C(2)—O(2) bonds, but no significant feature
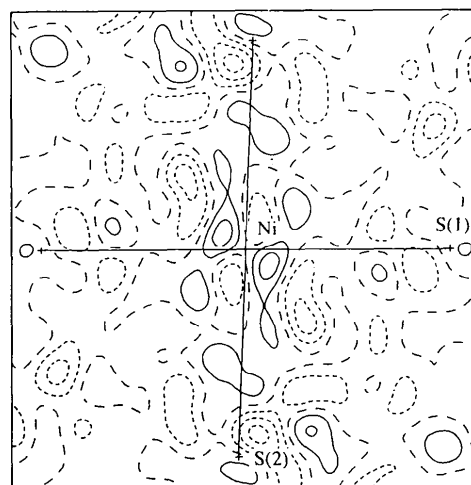
(*a*)

(*b*)

Fig. 3. (*a*) The difference density in the NiS₄ plane of K₂[Ni(S₂C₂O₂)₂] and, for comparison, (*b*) the difference density in the NiF₄ plane of KNiF₃. Contour interval is 0·2 e Å⁻³. Short dashed contour is negative; solid positive; long dash zero.
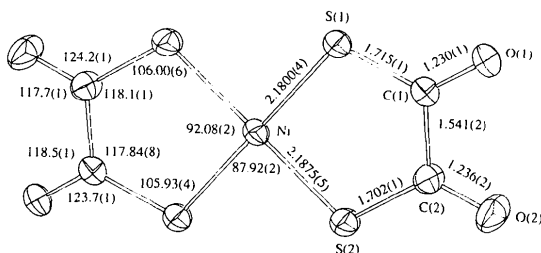
Fig. 1. Bond distances (Å) and angles (°) for the [Ni(S₂C₂O₂)₂] chromophore.

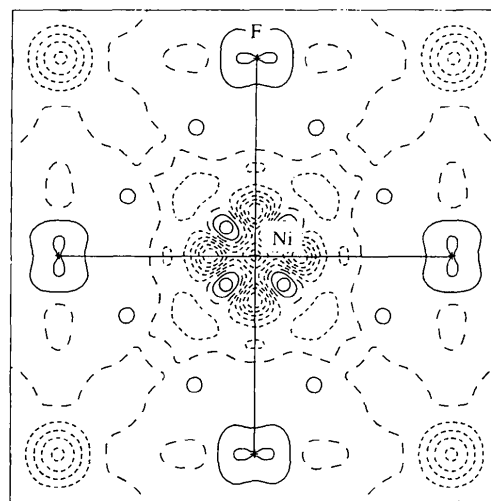Fig. 2. Diagram illustrating the pseudo-octahedral coordination of the Ni atom.

along the C(1)—O(1) bond. There are no prominent features near the different C—O bonds - a result which is also consistent with other studies (Dunitz & Seiler, 1983).

The electrostatic interaction energy is determined by the overlap of atoms. This quantity provides a good estimate of the experimental binding energy (Trefry, Maslen & Spackman, 1987). By evaluating the contributions for all atom–atom pairs one can identify the interactions which may contribute significantly to the binding energy. In so far as the polarization of the electron density is related to the strength of the atom–atom interactions, this also identifies the terms which may contribute significantly to the difference density.

The E_{es} were determined as functions of distance for all diatomic interactions in the structure. At any given Ni—O separation the interaction energy is much larger and more sharply varying than for the Ni—S interaction. However, the electron polarization associated with the Ni—O bond is large and energetically unfavourable when compared with the Ni—S interaction. This explains why the Ni—S bond forms in preference to the Ni—O bond.

In $Na_2Cu(CO_3)_2$ (Maslen, Spadaccini & Watson, 1986), the difference-density topology around the CuO_4 chromophore did not reflect the pseudo-four-fold symmetry of the structure. In the title compound the structure is more consistent with *mm* symmetry, with the pseudo-mirror planes bisecting the S(1)—Ni—S(2) angles, than with fourfold symmetry. The topology of the difference density (Fig. 3a) corresponds more closely to the ideal *mm* symmetry of the complete $[Ni(S_2C_2O_2)_2]$ moiety than it does to that of the NiS_4 chromophore. Thus the topography of the density is qualitatively consistent with the ideal molecular symmetry, although the magnitudes of the

Fig. 4. Difference density in a section containing Ni–Ni and Ni–K interactions. Contours as in Fig. 3.

corresponding features in the difference density are not exactly equal.

The polarization attributable to interaction between the Ni atom and its nearest neighbours is rather weak. The large regions of electron deficiency such as are observed for metal—F bonds do not occur in this structure. The difference in the difference-density topology along the Ni—S bonds for this compound and that for the Ni—F bonds of $KNiF_3$ is shown in Fig. 3(b). This change in density topography around the Ni atom is consistent with other studies. The ligating S atoms are less electronegative than F atoms. The weak polarization in this structure is expected because of the modest electronegativity and weak lone-pair development for the S atoms. There are actually small excesses of electrons along the Ni—S bonds, although their significance in the light of background noise is uncertain.

There is excess electron density in the directions along the pseudo-mirror planes but the density in the two planes differs in both magnitude and radial dependence. In Fig. 3(a), the peaks approximately 0·3 Å from Ni and 0·50 e Å^{-3} in height point directly at the midpoint of the C(1)—C(2) bond. The other pair of peaks (0·33 e Å^{-3}) are located approximately 0·7 Å from the Ni atom and point towards the open cell.

If features with such different characteristics can be equated, the difference density is qualitatively consistent with the pseudo-octahedral character of the structure. For octahedral coordination, the orbitals along the ⟨111⟩ directions of the octahedron are preferred. There is weak accumulation of density along these directions.

The difference density for this compound contains no strong or sharp features. This is not unexpected since we do not expect strong movement of electrons from the Ni—S overlap region. The degree of density polarization by the next-nearest neighbours depends strongly on the metal–ligand species. If the ligating atom is highly electronegative, the degree of movement of electrons into other regions of overlap is increased. This is particularly noticeable in the metal-oxide and metal-fluoride structures when the metal is at the upper end of the first transition series.

Difference-density features may also result from interaction with more distant atoms (Ni–Ni, Ni–K and K–K) but these are expected to be weak. The difference density in the plane containing the shortest Ni–Ni and Ni–K interaction vectors is illustrated in Fig. 4. That plane contains an Ni atom at a distance of 4·1949 (4) Å and two K atoms at distances of 4·5516 (6) and 5·5786 (6) Å. The positive features along the Ni–Ni vector are diffuse and located approximately 0·8 Å from Ni. The interaction between Ni atoms at this distance is expected to be small, as indicated by the low value for the electrostatic interaction energy ($E_{es} = -0·071$ eV).
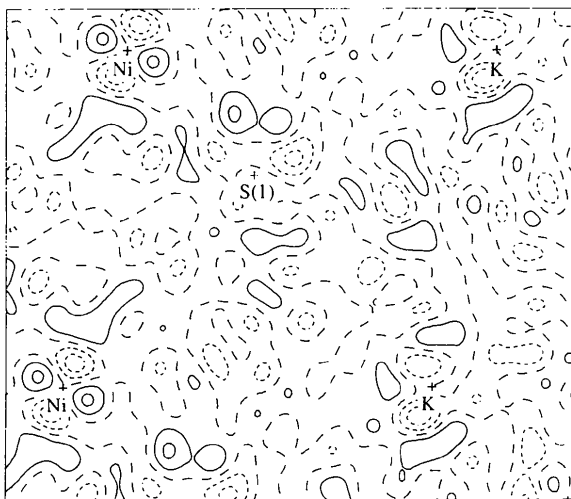
Table 3. *Net atomic charges* (e) *from the Hirshfeld partitioning of* $\Delta\rho$

Atom or group	Charge
Ni	−0·48 (2)
K	0·21 (3)
S(1)	0·01 (2)
S(2)	−0·07 (2)
O(1)	−0·06 (1)
O(2)	−0·16 (1)
C(1)	0·17 (1)
C(2)	0·14 (1)
$S_2C_2O_2$	0·03 (3)
NiS$_4$	−0·60 (3)

The Ni–K interaction is expected to be larger by virtue of greater overlap with the K atom. The electrostatic energy of interaction at 4·5516 Å is −0·111 eV, *i.e.* larger than that for the Ni–Ni interaction. There is a sharper peak 0·4 Å from the Ni atom along the Ni–K vector as shown in Fig. 4. The difference between these peaks is not in proportion to the difference in E_{es} but the density along the Ni–K vector is not entirely due to the K atom. The peak does not lie directly along the Ni–K vector because of the additional interactions. Given the complex nature of hybridization involving diffuse $4s$ orbitals and $3p$ orbitals in potassium, it is difficult to determine which orbital products these positive lobes represent.

Atomic charges

The effective atomic charges for this compound were determined using Hirshfeld partitioning of $\Delta\rho$. These results are given in Table 3. The atomic charges generally are lower than the formal charges and are concordant with the results of other workers (*e.g.* Hirshfeld & Hope, 1980). The charge of the K atom is consistent with the results for transition-metal fluorides and other alkali compounds reported by Bats & Fuess (1986). The charges obtained for the S, C and O atoms also reflect their electronegativities. The charges on the electropositive C atoms are similar and positive, while the electronegative O atoms have similar negative charges. The charges on the S atoms are small, reflecting their moderate electronegativity.

The Ni atom, however, is the most strongly polarized in this structure. The charge determined for Ni is −0·48 (2) e. That is, Ni is anionic. Whereas the charges on most metals are positive, the sign of the charge on a transition metal is a function of both the degree of occupancy of the $3d$ shell and the electronegativity of the ligating atoms. Any movement of electrons away from the region close to the Ni atom due to the S atoms is expected to be moderate. The density is enhanced due to the Ni–K interactions, and the Ni atom acquires a negative charge. Thus the Ni atom carries the major part of the charge associated with the $[Ni(S_2C_2O_2)_2]$ anion.

The appearance of the difference density suggests that the extra charge is concentrated in the d subshell. This implies that the free-atom configuration for Ni (d^8) is promoted towards d^9, which is Jahn–Teller unstable, and a square-planar or distorted octahedral structure should result. Thus the negative charge on the Ni atom is consistent with the geometry of the structure. More generally, it explains why, among the first-row transition series, Cu and Ni are favoured in square-planar structures. Where the $3d$ subshell in the free Cu atom is depleted of density, the d^{10} subshell adjusts towards the d^9 configuration. Where the $3d$ subshell of the nickel complex acquires additional density, the free-atom d^8 configuration moves towards the d^9 configuration, which is Jahn–Teller unstable.

References

ALCOCK, N. W. (1974). *Acta Cryst.* A30, 332–335.
BATS, J. W. & FUESS, H. (1986). *Acta Cryst.* B42, 26–32.
BECKER, P. J. (1977). *Phys. Scr.* 15, 119–142.
COPPENS, P., BOEHME, R., PRICE, P. F. & STEVENS, E. D. (1981). *Acta Cryst.* A37, 857–863.
COUCOUVANIS, D., BAENZIGER, N. C. & JOHNSON, S. M. (1973). *J. Am. Chem. Soc.* 95, 3075–3086.
COX, E. G., WARDLAW, W. & WEBSTER, K. C. (1935). *J. Chem. Soc.* pp. 1475–1480.
CROMER, D. T. & LIBERMAN, D. (1970). *J. Chem. Phys.* 53, 1891–1898.
CROMER, D. T. & MANN, J. B. (1968). *Acta Cryst.* A24, 321–324.
DUNITZ, J. D. & SEILER, P. (1983). *J. Am. Chem. Soc.* 105, 7056–7058.
GLEIZES, A., CLERY, F., BRUNIQUEL, M. F. & CASSOUX, P. (1979). *Inorg. Chim. Acta*, 37, 19–26.
GLEIZES, A., MAURY, F., CASSOUX, P. & GALY, J. (1981). *Z. Kristallogr.* 155, 293–306.
HIRSHFELD, F. L. & HOPE, H. (1980). *Acta Cryst.* B36, 406–415.
JONES, H. O. & TASKER, H. U. (1909). *J. Chem. Soc.* 95, 1904–1909.
KIJIMA, N., TANAKA, K. & MARUMO, F. (1981). *Acta Cryst.* B37, 545–548.
KIJIMA, N., TANAKA, K. & MARUMO, F. (1983). *Acta Cryst.* B39, 557–561.
LARSON, A. C. (1970). In *Crystallographic Computing*, edited by F. R. AHMED. Copenhagen: Munksgaard.
MASLEN, E. N., SPADACCINI, N. & WATSON, K. J. (1986). *Acta Cryst.* B42, 430–436.
MAURY, F. & GLEIZES, A. (1980). *Inorg. Chim. Acta*, 41, 185–194.
MIYATA, N., TANAKA, K. & MARUMO, F. (1983). *Acta Cryst.* B39, 561–564.
PAULI, W. (1925). *Z. Phys.* 31, 765.
ROBINSON, C. S. & JONES, H. O. (1912). *J. Chem. Soc.* 101, 62–76.
STEWART, J. M. & HALL, S. R. (1983). *The XTAL System of Crystallographic Programs*. Tech. Rep. TR-1364.1. Computer Science Centre, Univ. of Maryland, College Park, Maryland, USA.
TREFRY, M. G., MASLEN, E. N. & SPACKMAN, M. A. (1987). *J. Phys. C*, 20, 19–28.